RSC Advances

This is an *Accepted Manuscript*, which has been through the Royal Society of Chemistry peer review process and has been accepted for publication.

Accepted Manuscripts are published online shortly after acceptance, before technical editing, formatting and proof reading. Using this free service, authors can make their results available to the community, in citable form, before we publish the edited article. This *Accepted Manuscript* will be replaced by the edited, formatted and paginated article as soon as this is available.

You can find more information about *Accepted Manuscripts* in the Information for Authors.

Please note that technical editing may introduce minor changes to the text and/or graphics, which may alter content. The journal's standard Terms & Conditions and the Ethical guidelines still apply. In no event shall the Royal Society of Chemistry be held responsible for any errors or omissions in this *Accepted Manuscript* or any consequences arising from the use of any information it contains.

ROYAL SOCIETY OF CHEMISTRY

www.rsc.org/advances

Evaluation of corrosion protection properties of epoxy coating containing sol-gel surface modified nano-zirconia on mild steel

S. A. Haddadi[1], M. Mahdavian[2,*], E. Karimi[3]

[1]*Chemical and Petroleum Engineering Department, Sharif University of Technology, Tehran, Iran*

[2]*Surface Coating and Corrosion Department, Institute for Color Science and Technology, Tehran, Iran*

[3]*Materials Engineering Department, Sahand University of Technology, Tabriz, Iran*

Abstract

In this study, the effect of surface modified nano-zirconia (nano-ZrO_2) on the corrosion protection of epoxy coating on mild steel was investigated. An organosilane (trimethoxy methyl silane) was used as a surface modifier to improve the dispersability of the inorganic nanoparticles in the organic coating matrix. Fourier transform infrared spectroscopy (FTIR) and thermogravimetric analysis (TGA) were used to characterize the sol-gel surface modified nanoparticles. The dispersability of the modified and unmodified nano-zirconia in epoxy coating was examined by field emission-scanning electron microscopy (FE-SEM). Electrochemical impedance spectroscopy (EIS) and salt spray were employed to assess corrosion protection performance of the epoxy coatings. Results showed improved corrosion protection in the presence of the surface modified nanoparticles. Mechanical properties of the coatings were also found to be improved in the presence of modified nanoparticles in tensile and hardness measurements.

Keywords: *Nano-ZrO_2, Surface modification; Organosilane; Corrosion; Mild steel.*

* Corresponding author; E-mail: mahdavian-m@icrc.ac.ir, Tel: +982122969771, Fax: +982122947537

RSC Advances Accepted Manuscript

1. Introduction

The mild steel is wildly used in construction and many industries such as automotive, military, commercial machines, marine, oil and chemical industries as one of the most significant raw materials due to its good mechanical properties and low cost [1,2]. However, its corrosion resistance needs to be improved in corrosive environments. Organic coatings are generally used to provide higher corrosion resistance for mild steel. Organic resins based on epoxy, urethane, phenolic and vinyl ester are wildly used as a matrix in polymeric coating with high corrosive protection performance [3]. However, the corrosive agents such as oxygen, water and ions more or less can penetrate to all of the organic resin binders and cause metal-coating interface disbonding (adhesion loss) and corrosion [4,5]. It is shown that incorporation of corrosion inhibitors [6–8], anticorrosion pigments [9–11], adhesion promoters and surface modifiers [12–16] into the organic resin binders can improve the corrosion protection properties.

Nano composite polymeric coatings are have found great interest in the functional and high performance coatings [17]. It has been found that the inclusion of nano-fillers such as clay [19,36,37], titanium oxide (TiO_2) [32,38,39], silica (SiO_2) [40–43], silver oxide (Ag_2O) [44,45] and zirconia (ZrO_2) [4,37,46] could enhance corrosion protection due to the high surface area. However, application of inorganic nanoparticles in the organic coatings needs great care as the incompatibility could result in defects in the coatings. Organosilanes can be used as surface modifiers for inorganic nanoparticles [18,19]. They have a general chemical structure of $(RO)_3SiX$ where RO is a hydrolysable alkoxy group and X is an organofunctional group such as methacrylate, amine, epoxy and alkyl groups. It has been shown that silane functionalization of iron oxide and chromium oxide nanoparticles could greatly enhance the corrosion protection and mechanical properties of polyurethane coatings compared to the

RSC Advances Accepted Manuscript

unmodified nanoparticles [13,20,21]. Zirconia is well known for its excellent mechanical, physical and chemical properties [22–26]. This paper intends to study the effect of silane modification of nano-ZrO_2 on the corrosion protection properties of epoxy coating by means of electrochemical impedance spectroscopy (EIS) and salt spray.

2. Experimental

2.1- Materials

Epoxy resin (Epikote 828) and polyamine hardener (Epikure F205) were obtained to prepare epoxy coatings. Nano-zirconia was purchased from US-Nano Company with a particle size of 30-40 nm and purity of 99 %. Organosilane (trimethoxy methyl silane) was obtained from Aldrich with purity of 95 %.

The mild steel panels (St12) with the elemental composition shown in Table 1 were used as substrate.

Table 1

2.2- Surface modification of zirconia nanoparticles

In the first step, 90 mL ethanol was mixed with 5 mL water; then, 5 mL organosilane was added into mixture and stirred at 250 rpm for 24 h to perform hydrolysis reactions of silane agent at room temperature. The pH of hydrolysis step was adjusted at 2 with drop-by-drop addition of 1 M acetic acid solution. In the second step, 8 g nano-ZrO_2 was added into mixture. The pH was adjusted at 5.5 with drop-by-drop addition of 1 M ammonia solution and stirred at 350 rpm for 2.5 h to perform surface modification reaction in sol-gel route. In the third step, the mixture was centrifuged at 4000 rpm and residue was washed five times with DI water and dried in vacuum oven at 40 ºC for 72 h. The scheme of surface modification of zirconia nanoparticles has been shown in Fig. 1.

RSC Advances Accepted Manuscript

Figure 1

2.3- Preparation of coating samples

The nanocomposite coatings were prepared by direct mixing of 2 wt. % unmodified and modified ZrO_2 nanoparticles with epoxy resin by high speed mixer (3000 rpm) for 30 min after that, for complete dispersion of nanoparticles 45 cc of the mixture ultrasonicated for 5 min under condition of 90 W power, 25 kHz frequency, 1 min pulse on and 2 min pulse off. Ice-water bath was used for prevention of temperature rising during ultrasonication process. Also a blank epoxy resin containing no nanoparticle was prepared as a reference sample. As ultrasonication may lead to partial polymer chain scission, the blank epoxy resin was also ultrasonicated to ensure that all the conditions for comparison are the same expect pigment content. The mild steel plates (10 cm × 15 cm × 0.2 cm) abraded by emery papers no. 600, 800, and 1000 were cleaned by acetone. Then, the epoxy component containing unmodified and modified ZrO_2 nanoparticles were mixed with polyamine hardener at stoichiometric ratio (1:0.45 weight ratio of epoxy resin to polyamine). Immediately after mixing of epoxy coatings with hardener, the coating materials were applied on the cleaned mild steel substrates by a film applicator (Elcometer 3520 Baker). The coated steel plates remained at room temperature (25±5 ºC and 30±5 RH) for 12 h. To ensure complete curing, the plates were placed in an oven at 80 ºC for 2 h. The dry coatings thickness determined by Elcometer 456 was 25±3 µm. A surface area of 75±3 cm^2 of the coated mild steel plates was considered to expose salt spray while the rest area was sealed using a hot melt beeswax-colophony mixture. Coating was X-scribed before exposing salt spray. For EIS measurements, the exposed area to 3.5 wt. % NaCl solution was circular with diameter of 1 cm. Triplicates were prepared of each specimen type for EIS and salt spray measurements.

2.4- Techniques and analyses

RSC Advances Accepted Manuscript

To evaluate grafting of silane on the surface of ZrO_2 nanoparticles Fourier transform infrared spectroscopy (FTIR) was employed. FTIR was measured by Tensor 27 (Bruker, Germany) within wavenumber range of 400-4000 cm^{-1} using KBr pellet. Thermogravimetric (TG) analyzer L-801I (LINSEIS, Germany) was used under oxygen atmosphere within the temperature range of 25 to 800 ºC and heating rate of 10 ºC/min to evaluate the extent of silane grafting onto the nanoparticles.

A compactstat (Ivium, Netherland) was employed for electrochemical impedance spectroscopy (EIS) measurement on the coated specimens after exposure to 3.5 wt. % NaCl solution for 30 days. The measurements were conducted at open circuit potential (OCP), with 10 mV peak to peak perturbation within frequency range of 100 mHz–10 kHz. A three-electrode cell including Ag/ AgCl (3 M KCl) as a reference electrode, platinum as a working electrode and coated specimen as a working electrode was used to conduct EIS measurements. The Iviumsoft was used to analyze the EIS data. The corrosion protection performance of the coatings was also evaluated by salt spray exposure (ASTM B 117).

The mechanical properties of coatings were measured by the universal tensile machine Roell-Z010 (Zwick, Germany) at room temperature (24±3 ºC and 30±3 RH) with a loading rate of 1 mm/min. Vickers micro-hardness was also measured from the coatings at room temperature.

The dispersion of epoxy coating containing unmodified and modified nano-ZrO_2 and the morphology of the cross section of coatings were evaluated by field emission-scanning electron microscope (FE-SEM) Model Mira3 and energy dispersive X-ray (EDS) (Tescan, Czech Republic).

3. Result and Discussion

3.1- FTIR results

RSC Advances Accepted Manuscript

FTIR spectroscopy was used to evaluate silane grafting onto the surface of nano-ZrO_2. The unmodified and modified nano-ZrO_2 particles were placed in vacuum oven at 50 ºC for 24 h. The obtained spectra have been shown in Fig. 2. The assignments of the main FTIR bonds for unmodified and modified nano-ZrO_2 particles are tabulated in Table 2.

Figure 2

Fig. 2a shows the spectra of the unmodified nanoparticles. The main absorption bands at 514, 578 and 745 cm^{-1} are the characteristic peaks of Zr-O bonds in nano-ZrO_2 structures. The peaks at 2855 and 2960 cm^{-1} in spectrum of modified nanoparticles, Fig. 2(b) were assigned to asymmetric stretching of C-H in CH_3 section of the organosilane [5,13,21]. Also the absorption band observed at 1078 cm^{-1} could be assigned to Zr-O-Si bond on the surface modified nanoparticles [26]. In addition, the asymmetric vibration of Si-O-Si bond was appeared at 1181 cm^{-1} indicating successful grafting of silane onto the surface of the nanoparticles. The bending and stretching vibration of –OH groups were observed at 1630 and 3424 cm^{-1}, respectively which could be attributed to the adsorbed water on the surface [13,21]. The lower intensity of OH bending and vibration bands indicates lower water adsorption or higher hydrophobicity for the surface modified particles.

Table 2

3.2- TGA results

TGA themograms of unmodified and modified nano-ZrO_2 particles are shown in Fig. 3.

Figure 3

The weight loss was occurred in two stages. The first stage took place in temperature range of 40-200 ºC, the physically adsorbed water was evaporated. The weight loss attributed to this region was about 0.4 and 0.2 wt. % for unmodified and modified nano-ZrO_2 particles,

RSC Advances Accepted Manuscript

respectively. This result shows that modified nano-ZrO_2 powder has less tendencies to adsorb water molecules because of grafting of silane which made the surface more hydrophobic [13,26]. This result confirms the lower intensity of absorption bands related to O-H vibrations for the modified particles in the FTIR spectra. The second stage of weight loss was occurred in the temperature range of 200-690 ºC. The corresponding weight loss for untreated particle was about 1.3 wt. % which can be attributed to release of water molecules due to condensation reaction of hydroxyl groups on the surface of particles (dehydroxylation). However, the weight loss for modified particles was higher than unmodified particles which was about 2.3 wt. %. Beside dehydroxylation, thermal degradation of organic section of grafted silane onto the surface of the nano-ZrO_2 particles could take place in this region. Therefore, the extent of grafting could be estimated to 1 wt. % (2.3 – 1.3 wt. %) for the degradable section of the organosilane.

3.3- EIS results

The Nyquist plots obtained from EIS measurements for coated mild steel specimens immersed in 3.5 wt. % NaCl solution for 30 days have been displayed in Fig. 4.

Figure 4

The radius of semicircles in Nyquist plots, indicating impedance of coated electrodes are increased by addition of unmodified and modified ZrO_2 nanoparticles, respectively. The largest semicircle in Figure 4 is obtained for epoxy coating containing modified ZrO_2 nanoparticles.

The phase angle and impedance vs. frequency for coated specimens has been shown in Fig. 5.

Figure 5

RSC Advances Accepted Manuscript

According to Figure 5, the impedance at 100 mHz representing the performance of the specimen at near DC current condition is around 30 kOhm.cm^2, 400 kOhm.cm^2 and 40 MOhm.cm^2 for the blank epoxy coating, and the coatings containing unmodified and modified zirconia nanoparticles, respectively. In addition, the phase angle at 10 kHz is near -90 degree for epoxy coating containing modified nano-ZrO_2 particles. The most positive phase angle is obtained around -40 degree for the blank epoxy coating. It has been showed that when the current tends to pass through the coating capacitance at high frequency instead of coating resistance (due to high coating resistance), coating shows capacitive behavior where the phase angle of high frequency is near -90 degree. In contrast, when the current passes through the coating resistance (due to low coating resistance), coating shows resistive behavior where the phase angle at high frequencies shifts toward positive degrees [20,27,28]. Consequently, the coating containing modified nanoparticles showed the most capacitive behavior (best performance) among the coated samples.

Figure 6 shows the equivalent circuits used to fit EIS data for different coatings. In this figure, R_s, R_f, R_{ct}, CPE_{dl}, CPE_f and W represents solution resistance, film resistance, charge transfer resistance, constant phase element of double layer and that of deposited film and Warburg element, respectively. The used circuits in Fig. 6a and Fig. 6b represent a single-time constant behavior instead of a two-time constant behavior which is often associated with the porous polymeric coatings where corrosion takes place beneath the coating. Interestingly, although some of the coatings were deteriorated and rust spots were visible beneath the coatings, all the spectra save the blank coating's spectra, represented single time constant circuit. In addition, it was not possible to fit the spectra with two-time constant as there was large error for the fitted parameters. It seems that the time constant of coating was too close to that of corrosion; therefore, the coatings screened corrosion process electrochemically. The electrochemical parameters extracted from the EIS data are listed in Table 3.

RSC Advances Accepted Manuscript

Figure 6

Table 3

The Y_0 and n parameters presented in Table 3 are the CPE admittance and CPE exponent, respectively. According to the values of R_f listed in Table 3, inclusion of nanoparticles in the epoxy coating led to increase of coating film resistance, which could be related to the barrier effect of the nanoparticles. Considering the normal time-constant distribution, the effective coating capacitance (C_f) was calculated from the corresponding CPE parameters according to Eq. 1 [29].

$$C_f = \frac{(Y_0 R_f)^{\frac{1}{n}}}{R_f} \quad (1)$$

The C_f values derived from the above equation were 37.6, 0.29 and 0.21 nF/cm^2 for the epoxy coatings containing no nanoparticle, unmodified nanoparticle and modified nanoparticle, respectively. Considerable decrease of coating capacitance in the presence of modified nanoparticle could be related to the significant decrease in water penetration in the coating. Incompatibility of the particle and polymeric matrix may lead to defect formation at coating/particle interface. It seems that surface modified nanoparticles have better interaction with the epoxy matrix compared to the unmodified nanoparticles.

3.4- Salt spray exposure

The appearance of the epoxy coating samples after 240 h of exposure to salt spray are shown in Fig. 7.

Figure 7

It is clear from Fig. 7 that the corrosion protection of epoxy coatings increased due to addition of nanoparticles to epoxy coating. The surface modification of nanoparticles

RSC Advances Accepted Manuscript

considerably improved the corrosion protection properties of the epoxy coating in comparison with unmodified nanoparticles. Disbonded coating was removed by a sharp blade, and the delaminated area of the coatings was tabulated in Table 4.

Table 4

The delamination area of the coatings from mild steel substrates decreased by addition of nanoparticles in the epoxy coatings. The epoxy coating containing modified nano-ZrO_2 particles has the lowest delamination from mild steel probably due to less water penetration in the coating observed in the EIS results. The salt spray exposure results are in good agreement with EIS results where the addition of nanoparticles, especially surface modified one, greatly increased the corrosion protection performance in immersion condition.

3.5- Tensile test results

The surface modification of the nanoparticles can change the surface chemistry and consequently alters their interactions and compatibility with the polymer coating matrix. The change in compatibility of particle and polymer not only affects the corrosion protection performance but also the mechanical properties. The mechanical properties could readily show the change in the interaction of filler and matrix. Therefore, epoxy coating materials prepared according to the mentioned method (see section 2.3) were casted in a wooden mold (ASTM D-628) prepared by laser machine. After casting of epoxy coating material, the filled wooden mold was placed in vacuum oven at 100 ºC for 1 h to cure. Triplicates were prepared for each specimen. Figure 8 shows the tensile specimens after fracture.

Figure 8

The results of tensile test (stress-strain curve) from the blank epoxy and epoxy containing unmodified and modified nanoparticles have been shown in Fig. 9.

RSC Advances Accepted Manuscript

Figure 9

As showed in Fig. 9, the surface modification of nanoparticles influenced the mechanical properties of the epoxy coating effectively. The energy at break and maximum load of the epoxy coating are listed in Table 5.

Table 5

According to Table 5, incorporation of unmodified nanoparticles in epoxy coating considerably improved the mechanical properties. Incorporation of unmodified nanoparticles had limited impact on mechanical behavior of the epoxy coating. According to Fig. 9, by addition of modified nanoparticles in epoxy a transition from brittle to tough behavior occurs. Grafting silane structure onto the particles surface increases the physical interaction between particles and matrix dramatically. In addition, ZrO_2 nanoparticles have high fracture toughness; consequently, they can increase the epoxy toughness where the particle and matrix are highly compatible.

3.6- Vickers hardness

The hardness measurement test was performed for determining the hardness values of epoxy coatings. The results are shown in Fig. 10.

Figure 10

The results show the hardness values of the epoxy coatings increased due to addition of nanoparticles with high elastic modulus of solid contents compared to polymeric matrix. Higher hardness of the sample composed of modified nanoparticles compared to the one containing unmodified nanoparticles could be related to the better compatibility of the particle with the polymer resulting in less week points and defects in the coating.

3.7- FE-SEM

RSC Advances Accepted Manuscript

The cross-sectional images of the coating from the near top, middle and near bottom areas are shown in Fig. 11.

Figure 11

The cross-section of the coating containing unmodified nanoparticle reveals considerable differences in the particles distribution across the coating thickness (see Fig. $11a_1$, b_1 and c_1). The micrographs clearly show high concentration of zirconia nanoparticle near top of the coatings. Also, the unmodified nanoparticles tend to form agglomerates in the coatings which reflects their incompatibility with the coating matrix. The FE-SEM micrographs from the coatings containing modified nanoparticles show no agglomeration of the nanoparticles across the coating thickness. No considerable difference in the particles distribution across the coating thickness could be observed in the cross-section image of the coating containing modified nanoparticle (see Fig. $11a_2$, b_2 and c_2). It seems that surface modification resulted in uniform distribution of particles in the coatings which reflects enhanced nanoparticles compatibility with the coating matrix.

The zirconia weight percentage obtained from EDS analysis for the corresponding FE-SEM images are depicted in Fig. 12.

Figure 12

According to Fig. 12, unmodified zirconia nanoparticles tends to migrate to the coating/air interface. It seems that the unmodified nanoparticles tend to migrate to the surface due to incompatibility with the coating matrix. The EDS results from the coating containing modified nanoparticles show uniform distribution of particles across the coating thickness.

The fracture morphology of the coatings is shown in Fig. 13. Evaluation of fracture morphology of coating containing unmodified and modified nano-ZrO_2 particles could

RSC Advances Accepted Manuscript

indicate brittle or tough behavior of the coatings. The micro ruptures present at the fractured surface of the coating containing unmodified nanoparticles in Fig. 13a; however, for the coating containing modified nanoparticles the size of micro ruptures are reduced (Fig. 13b). The better dispersion (lower aggregates and agglomerates) of modified nanoparticle than the unmodified one in epoxy coating provides more sites for stress concentration which results in better dissipation of energy during stress application. These observations confirm that the use of modified nanoparticles makes the coating tougher as shown in tensile test.

Figure 13

4. Conclusion

The anticorrosion performance of the epoxy coating containing unmodified and modified ZrO_2 nanoparticles with trimethoxy methyl silane on mild steel substrate was investigated. The results are summarized as follow:

- FTIR and TGA results showed that silane was successfully grafted onto the surface of ZrO_2 nanoparticles.
- Results of the salt spray and EIS measurements revealed that the epoxy coating modified with nanoparticle provided better corrosion protection performance compared with the blank epoxy coating. The highest corrosion protection was observed for the coating containing modified nanoparticles.
- Inclusion of unmodified nanoparticles in the epoxy coating increased the mechanical properties compared to the blank epoxy coating. The epoxy coating containing modified nanoparticles showed superior hardness, energy at break and maximum load among the examined specimens. Also incorporation of modified nanoparticles led to a change from brittle to tough behavior.

RSC Advances Accepted Manuscript

- SEM micrographs from fracture surface showed a proper dispersion of surface modified particles in the epoxy matrix and the great tendency of unmodified particle for agglomeration.
- Surface modification of nano-zirconia pigments improved mechanical and corrosion protection performance of the epoxy coatings. Therefore, surface modified nano-zirconia could be possible choice for high performance epoxy coatings formulations.

References

1 I. Ahamad, R. Prasad and M. A. Quraishi, *Corrosion Science*, 2010, 52, 3033–3041.

2 M. Gao, X. Zeng, J. Yan and Q. Hu, *Applied Surface Science*, 2008, 254, 5715–5721.

3 A. Forsgren, *Corrosion control through organic coatings*, Tylor & Francis (CRC Press), Abington (USA), 2006.

4 M. Mahdavian, R. Naderi, M. Peighambari, M. Hamdipour and S. a. Haddadi, *Journal of Industrial and Engineering Chemistry*, 2014.

5 M. Pantoja, B. Diaz-Benito, F. Velasco, J. Abenojar and J. C. del Real, *Applied Surface Science*, 2009, 255, 6386–6390.

6 V. Moutarlier, B. Neveu and M. P. Gigandet, *Surface and Coatings Technology*, 2008, 202, 2052–2058.

7 a. C. Balaskas, I. a. Kartsonakis, D. Snihirova, M. F. Montemor and G. Kordas, *Progress in Organic Coatings*, 2011, 72, 653–662.

8 H. Wang and R. Akid, *Corrosion Science*, 2008, 50, 1142–1148.

9 A. Kalendová, D. Veselý, I. Sapurina and J. Stejskal, *Progress in Organic Coatings*, 2008, 63, 228–237.

10 F. Askari, E. Ghasemi, B. Ramezanzadeh and M. Mahdavian, *Dyes and Pigments*, 2014, 109, 189–199.

11 E. Alibakhshi, E. Ghasemi and M. Mahdavian, *Progress in Organic Coatings*, 2013, 76, 224–230.

12 J. P. Matinlinna, M. Ozcan, L. V. J. Lassila and P. K. Vallittu, *Dental materials : official publication of the Academy of Dental Materials*, 2004, 20, 804–13.

13 M. J. Palimi, M. Rostami, M. Mahdavian and B. Ramezanzadeh, *Progress in Organic Coatings*, 2014, 77, 1663–1673.

RSC Advances Accepted Manuscript

14 R. Zandi Zand, K. Verbeken and A. Adriaens, *Progress in Organic Coatings*, 2011, 72, 709–715.

15 W.-G. Ji, J.-M. Hu, L. Liu, J.-Q. Zhang and C.-N. Cao, *Surface and Coatings Technology*, 2007, 201, 4789–4795.

16 D. D. Rodrigues and J. G. Broughton, *International Journal of Adhesion and Adhesives*, 2013, 46, 62–73.

17 Y. Yu, J. Yeh, S. Liou, C. Chen, D. Liaw and H. Lu, *Journal of applied polymer science*, 2004, 92, 3573–3582.

18 K. L. Mittal, *Silanes and other coupling agents*, Tylor & Francis (CRC Press), Florida (USA), 2007, vol. 4.

19 A. A. Tracton, *Coatings technology handbook*, Tylor & Francis (CRC Press), Florida (USA), Third Edit., 2010.

20 M. J. Palimi, M. Rostami, M. Mahdavian and B. Ramezanzadeh, *Progress in Organic Coatings*, 2014, 77, 1935–1945.

21 M. J. Palimi, M. Rostami, M. Mahdavian and B. Ramezanzadeh, *Applied Surface Science*, 2014, 320, 60–72.

22 C. J. Howard, R. J. Hill and B. E. Reichert, *Acta Crystallographica Section B: Structural Science*, 1988, 44, 116–120.

23 K. Izumi, M. Murakami, T. Deguchi, A. Morita, N. Tohge and T. Minami, *Journal of the American Ceramic Society*, 1989, 72, 1465–1468.

24 W. Q. Wang, C. K. Sha, D. Q. Sun and X. Y. Gu, *Materials Science and Engineering: A*, 2006, 424, 1–5.

25 G. Teufer, *Acta Crystallographica*, 1962, 15, 1187.

26 M. Behzadnasab, S. M. Mirabedini, K. Kabiri and S. Jamali, *Corrosion Science*, 2011, 53, 89–98.

27 M. Akbarian, M. E. Olya, M. Mahdavian and M. Ataeefard, *Progress in Organic Coatings*, 2014, 77, 1233–1240.

28 M. Mahdavian and M. M. Attar, *Corrosion Science*, 2006, 48, 4152–4157.

29 B. Hirschorn, M. E. Orazem, B. Tribollet, V. Vivier, I. Frateur and M. Musiani, *Electrochimica Acta*, 2010, 55, 6218–6227.

RSC Advances Accepted Manuscript

Figure Captions:

Figure 1: The scheme of surface modification of a zirconia nanoparticle

Figure 2: FTIR results of (a): unmodified- (b): modified nano-ZrO_2 powder

Figure 3: TGA thermograms of unmodified and modified nano-ZrO_2 particles

Figure 4: The Nyquist plots for (▲) blank epoxy coating; (■) epoxy coating containing unmodified nano-ZrO2 particles and (♦) epoxy coating containing modified nano-ZrO2 particles (the measured data points are displayed by symbols and the fitted curve by the equivalent electrical circuits of Fig. 6 are shown by continuous lines)

Figure 5: The phase angle (a) and impedance (b) Bode plots for (▲) blank epoxy coating; (■) epoxy coating containing unmodified nano-ZrO_2 particles and (♦) epoxy coating containing modified nano-ZrO_2 particles (the measured data points are displayed by symbols and the fitted curve by the equivalent electrical circuits of Fig. 6 are shown by continuous lines)

Figure 6: The equivalent electrical circuits used to fit (a) epoxy coating containing modified nano-ZrO_2 particles, (b) epoxy coating containing unmodified nano-ZrO_2 particles, (c) blank epoxy coating

Figure 7: The appearance of (a) the blank coating, (b) epoxy containing unmodified nanoparticles and (c) epoxy containing modified nanoparticles after 240 h of exposure to salt spray

Figure 8: The tensile specimens after fracture

Figure 9: The tensile plots of (a) blank epoxy, (b) epoxy filled with unmodified ZrO_2 nanoparticles and (c) epoxy filled with modified ZrO_2 nanoparticles

Figure 10: The hardness values of (a) blank epoxy coating, (b) epoxy coating containing unmodified ZrO_2 nanoparticles and (c) epoxy coating containing modified ZrO_2 nanoparticles

Figure 11: cross-sectional images of epoxy coating containing unmodified nano-ZrO_2 from near top (a_1), middle (b_1) and near bottom (c_1) areas and epoxy coating containing modified nano-ZrO_2 from near top (a_2), middle (b_2) and near bottom (c_2) areas

RSC Advances Accepted Manuscript

Figure 12: The weight percentage of Zr at top, middle and bottom of the coating. The rest of elements analyzed were C, O and N

Figure 13: The fracture morphology of epoxy coating containing unmodified (a) and modified (b) nano-ZrO_2 obtained by FE-SEM

RSC Advances Accepted Manuscript

Table 1: Composition of the mild steel substrate

element	Fe	C	Mn	P	S	Others
Wt.%	99.09	0.12	0.6	0.045	0.045	≤ 0.1

RSC Advances Accepted Manuscript

Table 2: Characteristic absorption peaks obtained from FTIR spectrum of unmodified and modified nano-ZrO_2

No.	Functionality	Wavenumber/ cm^{-1} (Unmodified ZrO_2)	Wavenumber/ cm^{-1} (Modified ZrO_2)
1	Zr-O	514, 578, 745	514, 578, 745
2	Zr-OH	3424	3424
3	Zr-O-Si	-	1078
4	-OH bending	1630	1630
5	-OH stretching	3424	3424
6	Asymmetric Stretching C-H	-	2855, 2960
7	Si-O-Si	-	1181

RSC Advances Accepted Manuscript

Table 3: The electrochemical parameters extracted from the EIS data

Coating Type	$Y_{0,f}$ ($s^n\ \Omega^{-1}\ cm^{-2}$)	n_f	R_f ($\Omega\ cm^2$)	$Y_{0,dl}$ ($s^n\ \Omega^{-1}\ cm^{-2}$)	n_{dl}	R_{ct} ($\Omega\ cm^2$)
Blank epoxy	$3.7\times10^{-7}\pm1\times10^{-8}$	0.67±0.01	26144±105	$7.2\times10^{-4}\pm2\times10^{-5}$	0.81±0.02	$2.0\times10^{4}\pm1\times10^{3}$
Epoxy containing unmodified ZrO_2 [a]	$2.4\times10^{-9}\pm3\times10^{-10}$	0.77±0.02	$3.8\times10^{5}\pm1.8\times10^{4}$	-	-	-
Epoxy containing modified ZrO_2	$3.4\times10^{-10}\pm2\times10^{-11}$	0.90±0.02	$3.9\times10^{7}\pm1.1\times10^{6}$	-	-	-

[a] Warburg parameter for the epoxy coating containing unmodified ZrO_2 was $1.4\times10^{9} \pm 2.4\times10^{8}$ ($s^{0.5}\ \Omega^{-1}\ cm^{-2}$)

RSC Advances Accepted Manuscript

Table 4: The delamination percentage of the coatings after 240 h exposure to salt spray

Coating	Blank epoxy coating	Epoxy coating containing unmodified nanoparticles	Epoxy coating containing modified nanoparticles
delamination %	55	41	24

RSC Advances Accepted Manuscript

Table 5: The energy at break and maximum load of unpigmented and pigmented epoxy coatings

Coating type	Energy at break ($MN.m^{-2}$)	Elongation at break (ε_B)/ %	Maximum load (σ_B)/ MPa
Blank epoxy	76	4.2	26
Epoxy containing unmodified ZrO_2	125.2	6	31
Epoxy containing modified ZrO_2	301.7	10.1	30

RSC Advances Accepted Manuscript

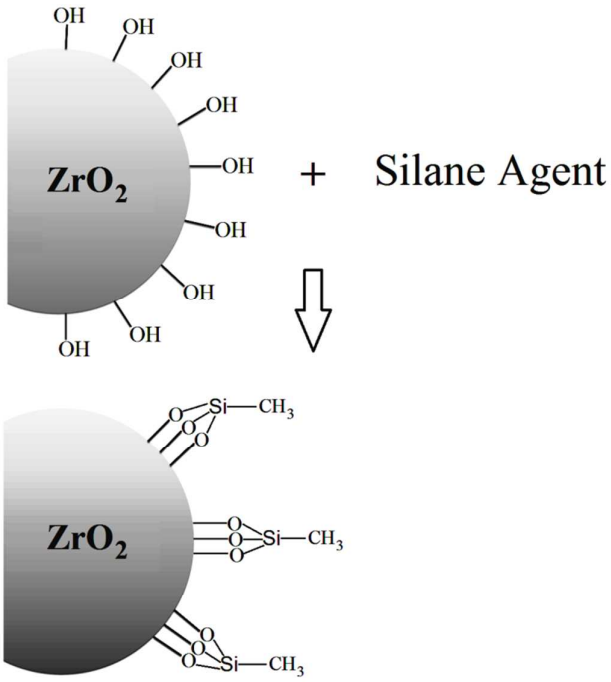

Figure 1: The scheme of surface modification of a zirconia nanoparticle

RSC Advances Accepted Manuscript

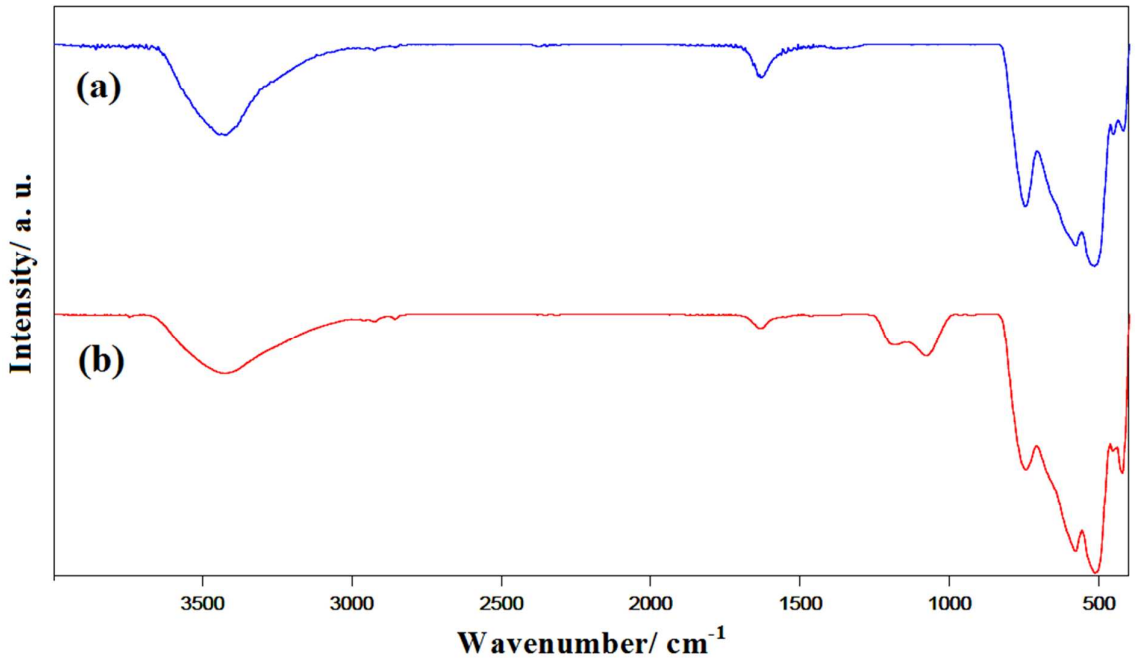

Figure 2: FTIR results of (a): unmodified- (b): modified nano-ZrO_2 powder

RSC Advances Accepted Manuscript

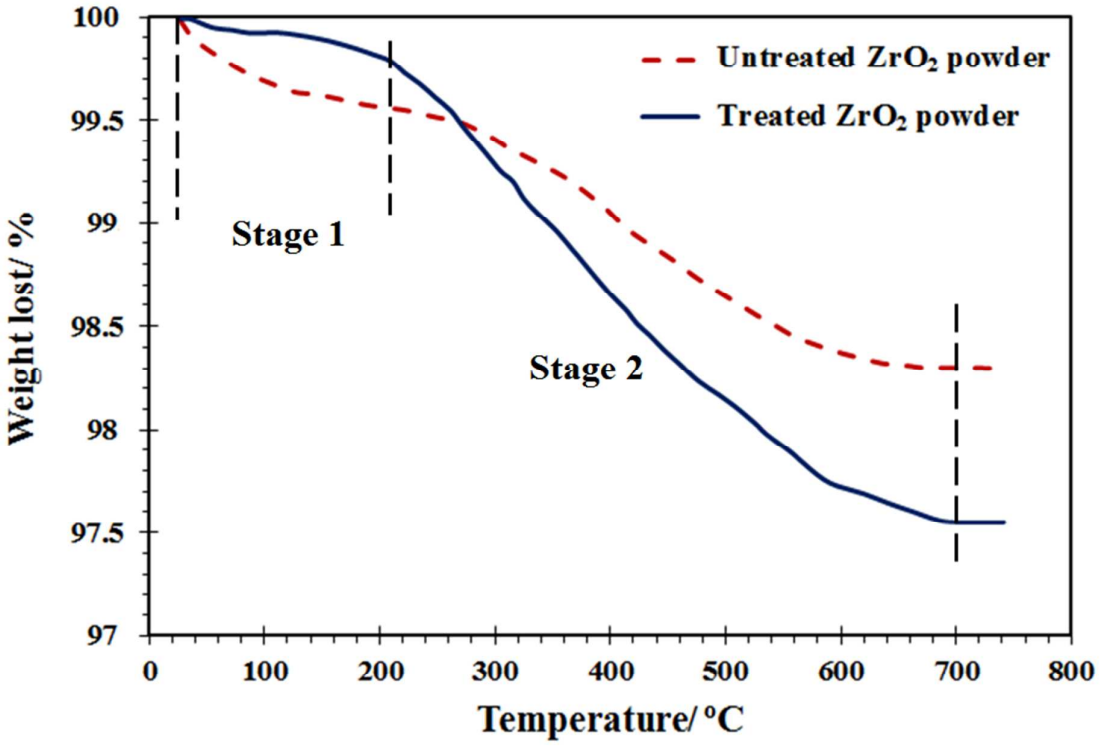

Figure 3: TGA thermograms of unmodified and modified nano-ZrO_2 particles

RSC Advances Accepted Manuscript

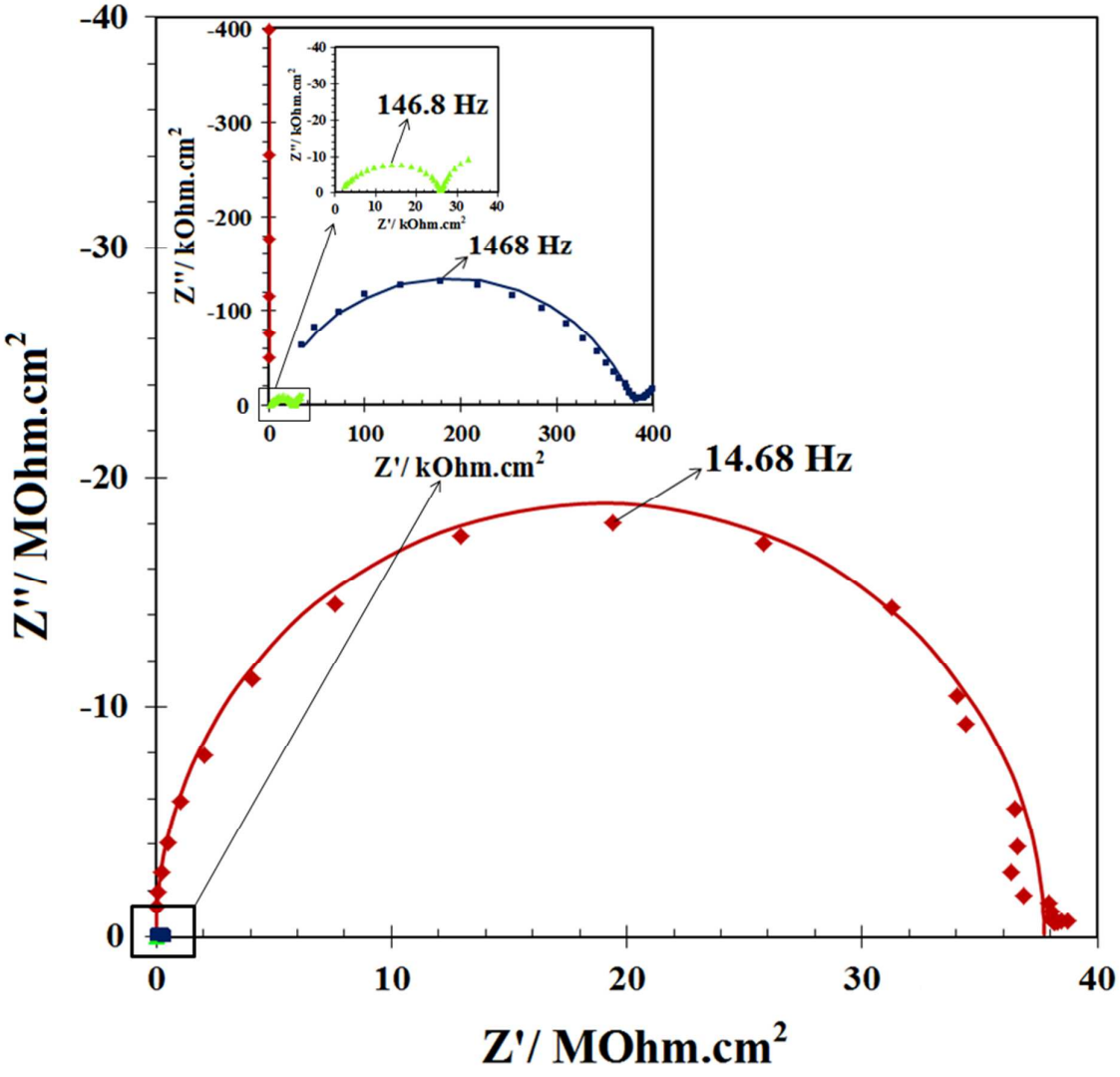

Figure 4: The Nyquist plots for (▲) blank epoxy coating; (■) epoxy coating containing unmodified nano-ZrO2 particles and (♦) epoxy coating containing modified nano-ZrO2 particles (the measured data points are displayed by symbols and the fitted curve by the equivalent electrical circuits of Fig. 6 are shown by continuous lines)

RSC Advances Accepted Manuscript

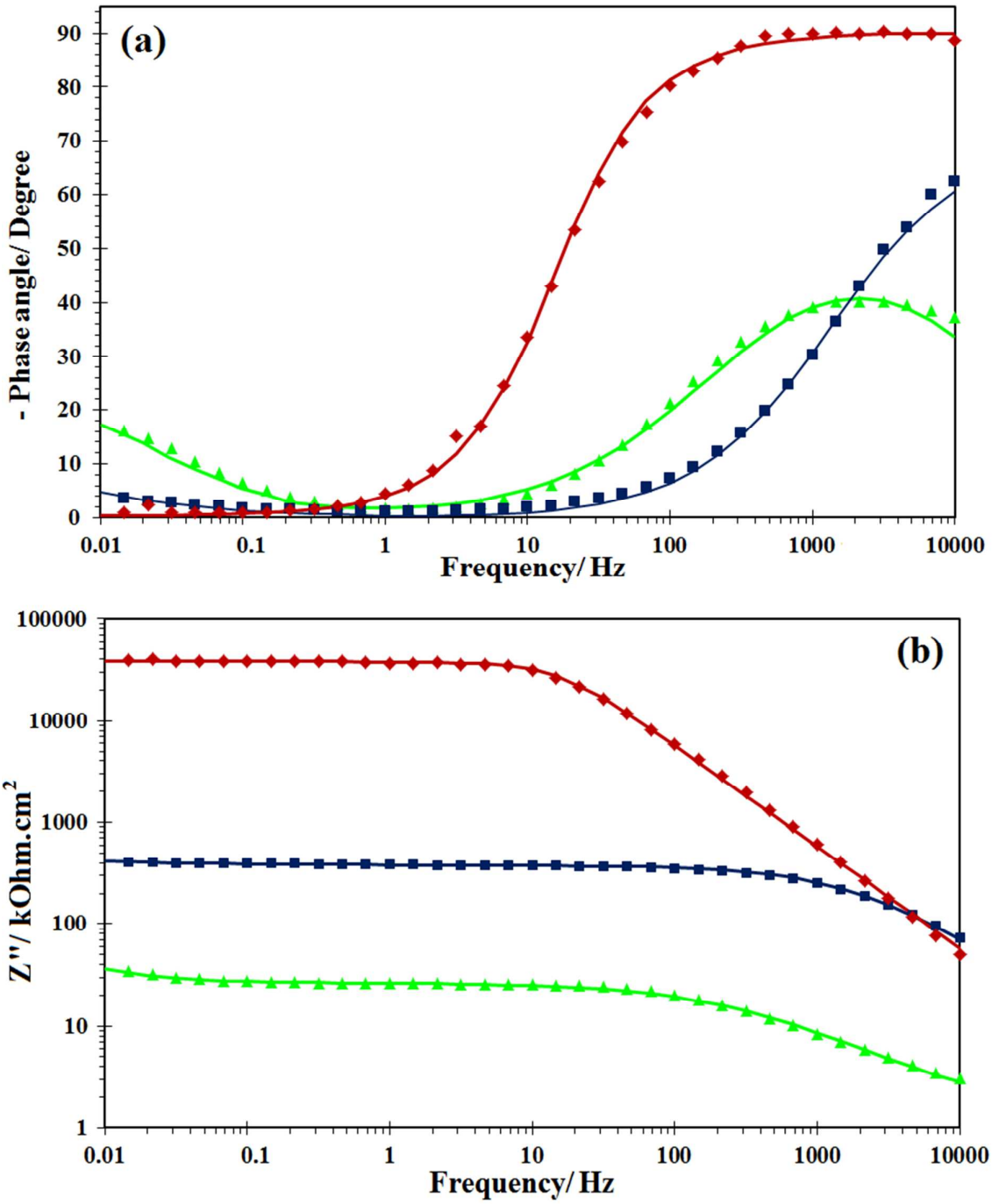

Figure 5: The phase angle (a) and impedance (b) Bode plots for (▲) blank epoxy coating; (■) epoxy coating containing unmodified nano-ZrO_2 particles and (♦) epoxy coating containing modified nano-ZrO_2 particles (the measured data points are displayed by symbols and the fitted curve by the equivalent electrical circuits of Fig. 6 are shown by continuous lines)

RSC Advances Accepted Manuscript

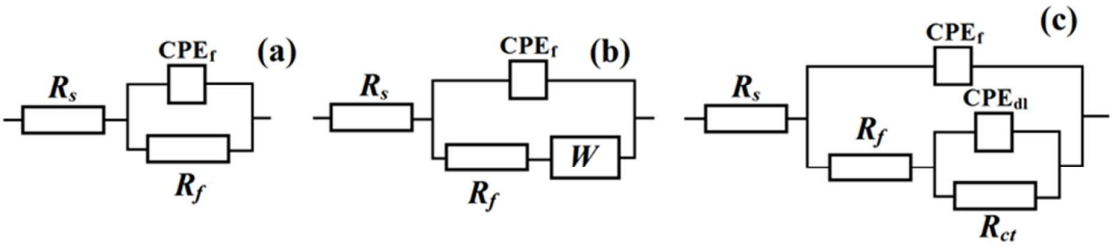

Figure 6: The equivalent electrical circuits used to fit (a) epoxy coating containing modified nano-ZrO_2 particles, (b) epoxy coating containing unmodified nano-ZrO_2 particles, (c) blank epoxy coating

RSC Advances Accepted Manuscript

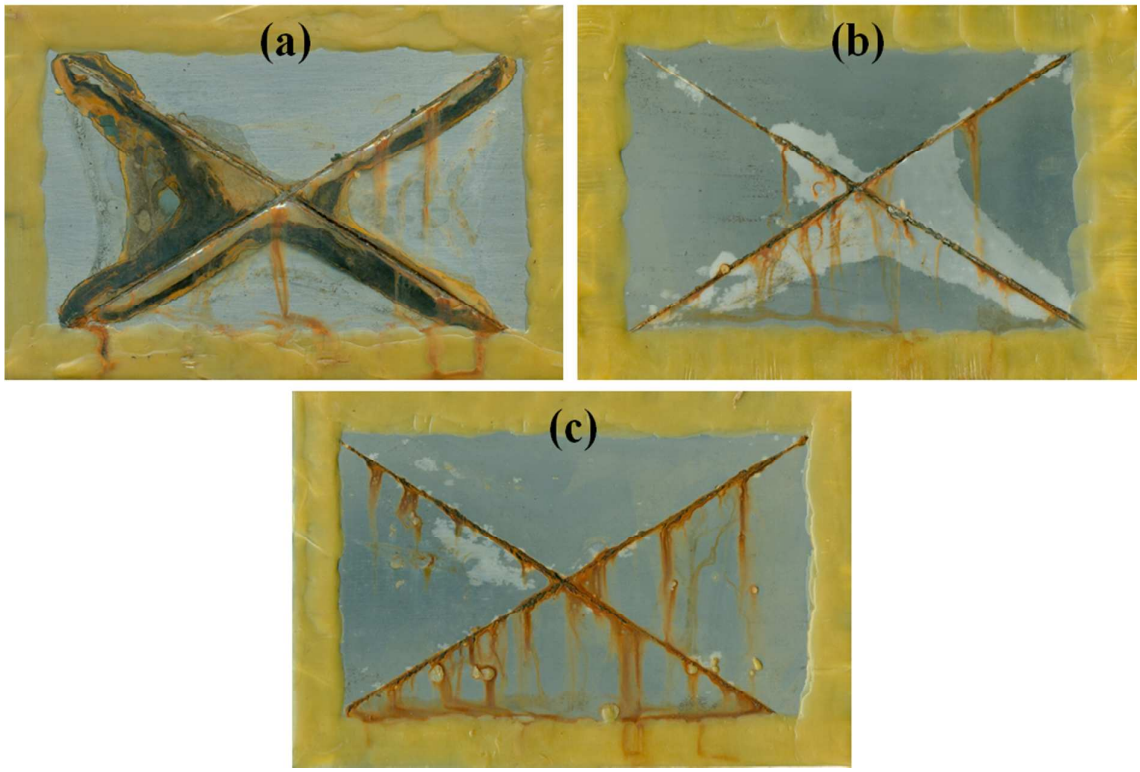

Figure 7: The appearance of (a) the blank coating, (b) epoxy containing unmodified nanoparticles and (c) epoxy containing modified nanoparticles after 240 h of exposure to salt spray

RSC Advances Accepted Manuscript

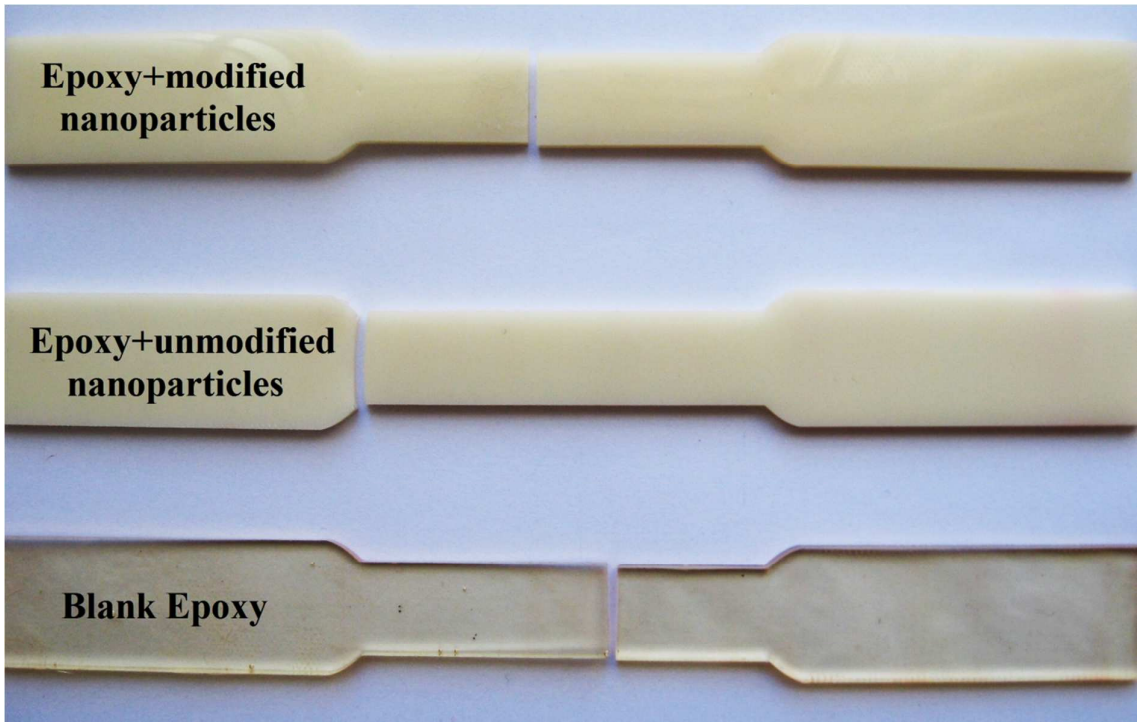

Figure 8: The tensile specimens after fracture

RSC Advances Accepted Manuscript

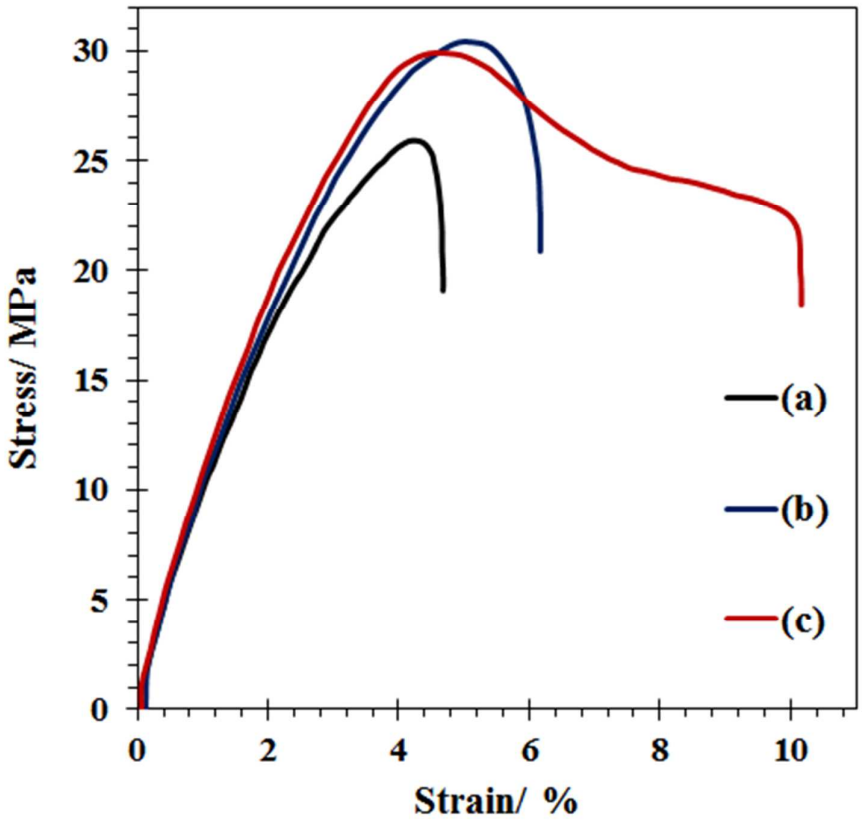

Figure 9: The tensile plots of (a) blank epoxy, (b) epoxy filled with unmodified ZrO_2 nanoparticles and (c) epoxy filled with modified ZrO_2 nanoparticles

RSC Advances Accepted Manuscript

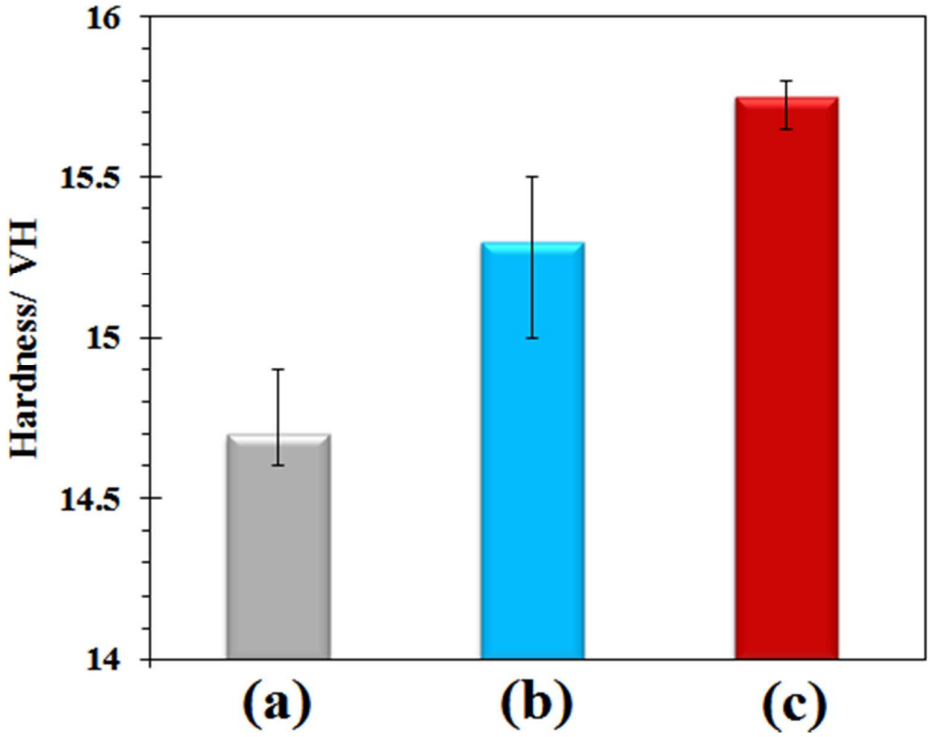

Figure 10: The hardness values of (a) blank epoxy coating, (b) epoxy coating containing unmodified ZrO_2 nanoparticles and (c) epoxy coating containing modified ZrO_2 nanoparticles

RSC Advances Accepted Manuscript

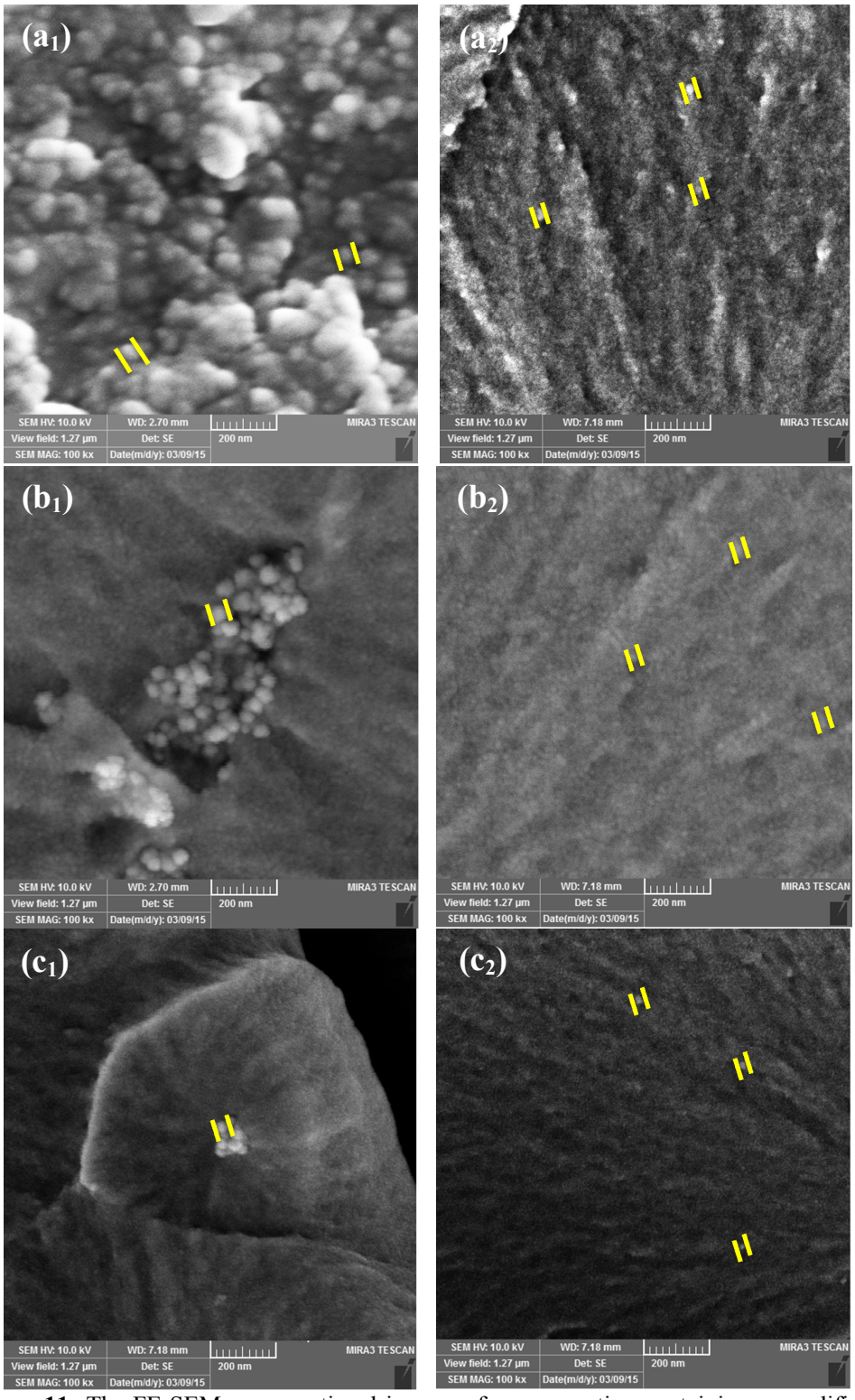

Figure 11: The FE-SEM cross-sectional images of epoxy coating containing unmodified nano-ZrO_2 from near top (a_1), middle (b_1) and near bottom (c_1) areas and epoxy coating containing modified nano-ZrO_2 from near top (a_2), middle (b_2) and near bottom (c_2) areas.

RSC Advances Accepted Manuscript

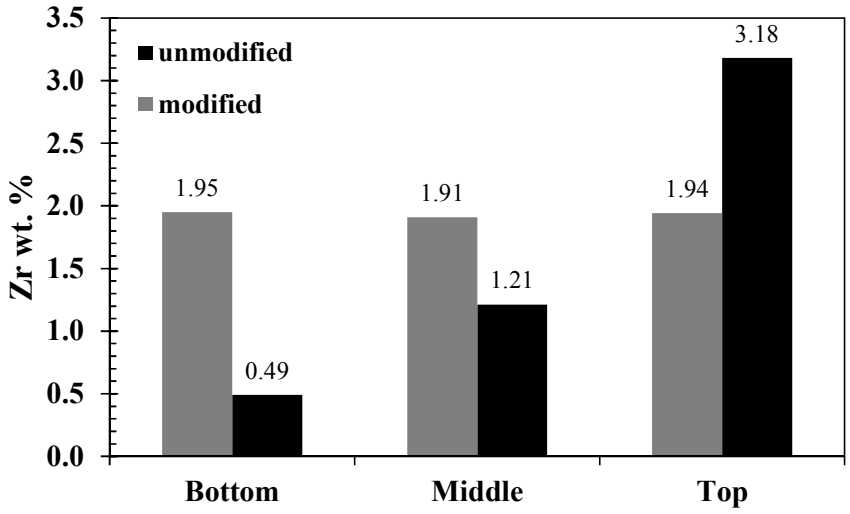

Figure 12: The weight percentage of Zr at top, middle and bottom of the coating. The rest of elements analyzed were C, O and N.

RSC Advances Accepted Manuscript

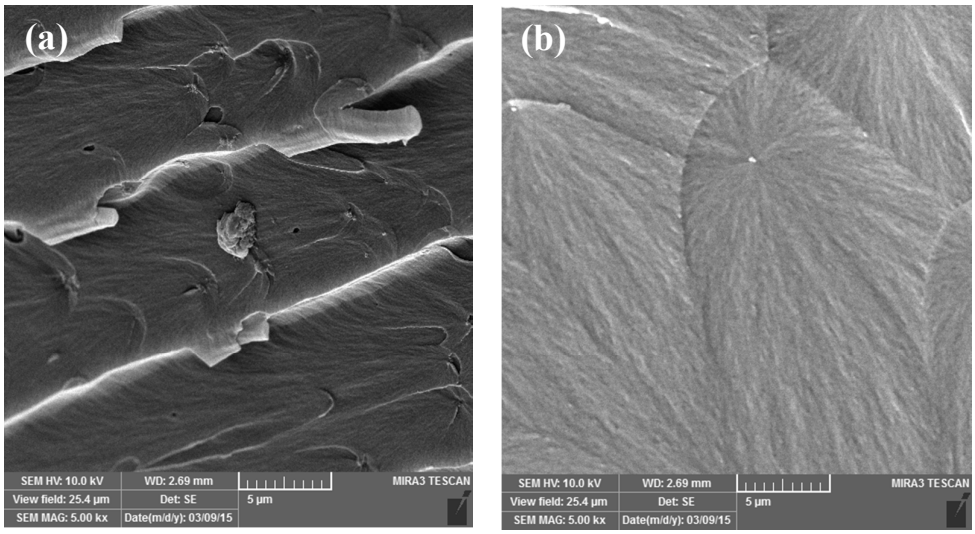

Figure 13: The fracture morphology of epoxy coating containing unmodified (a) and modified (b) nano-ZrO_2 obtained by FE-SEM.

RSC Advances Accepted Manuscript